



ELSEVIER

Contents lists available at ScienceDirect

Journal of Organometallic Chemistry

journal homepage: www.elsevier.com/locate/jorgancem



DFT study of alkene hydrogenation catalyzed by Rh(acac)(CO)₂

Xiangai Yuan, Siwei Bi ^{*}, Yangjun Ding, Lingjun Liu, Min Sun

College of Chemistry and Chemical Engineering, Qufu Normal University, Qufu, Shandong 273165, China

ARTICLE INFO

Article history:

Received 14 January 2010

Received in revised form 9 March 2010

Accepted 12 March 2010

Available online 16 March 2010

Keywords:

Hydrogenation

Alkene

Rh(acac)(CO)₂

Density functional calculation

ABSTRACT

Hydrogenation of alkene catalyzed by the catalyst Rh(acac)(CO)₂ has been investigated theoretically with the aid of density functional calculations. The findings are as follows: (1) An associative but not a dissociative mechanism is found favorable for substitution of a carbonyl by ethene. (2) The substitution step of a carbonyl by H₂ is found to be involved prior to the oxidative addition of H₂, and this step is predicted to be the rate-determining step. (3) The ethene inserts into the Rh–H trans to CO but not the one cis to CO. (4) Reductive elimination of ethane occurs directly from a five-coordinate intermediate where the hydride but not the ethyl group occupies the apical position of the square-pyramidal structure. Some other issues related to the reactions are also discussed.

© 2010 Elsevier B.V. All rights reserved.

1. Introduction

The hydrogenation of alkenes catalyzed by transition metal complexes is a kind of very important reactions [1–16] and an atom-economical synthetic methodology which has been used extensively in academic and industrial settings [17]. Alkene complexes of transition metals [18–24] play an important role in understanding the reaction mechanisms for hydrogenation of alkenes, which has been confirmed experimentally and theoretically to proceed via a wide variety of different pathways [25–30]. Rhodium (I) complexes with bidentate β -diketonato ligands are well-known catalysts for hydrogenation of alkene and are also used for hydroformylation of olefin [31–34]. Rh(acac)(CO)₂ (acac = acetylacetonato) is among the most common. Bonati and Wilkinson first reported the complex Rh(acac)(CO)₂ and its substitution reaction with olefin in 1964 [35]. To our knowledge, there have been few reports [36] of using Rh(acac)(CO)₂ solely as a hydrogenation catalyst, and theoretical studies on alkene hydrogenation catalyzed by Rh(acac)(CO)₂ are little reported.

In 2003, Poliakoff and co-workers studied the hydrogenation of alkene catalyzed by Rh(acac)(CO)₂ in a polyethylene film through FTIR either in the presence of high-pressure hydrogen at 273 K, and proposed a catalytic cycle (Scheme 1) for the reaction [37]. Several steps were involved in the proposed catalytic cycle, step (1): CO dissociation, step (2): alkene coordination, step (3): oxidative addition of H₂, step (4): insertion of the coordinated alkene into M–H, step (5): reductive elimination of the product. What we are interested in and attempt to study are as follows. (i) For

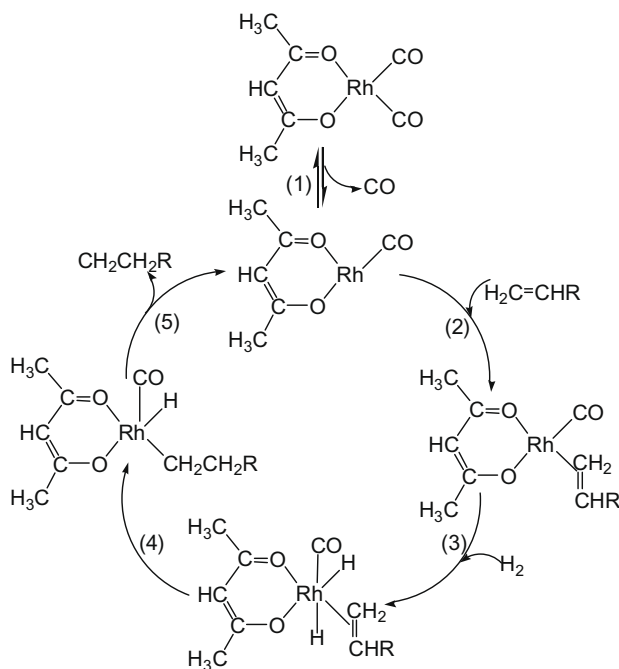
substitution of CO by alkene, one possible path is through the dissociative mechanism as shown by steps (1) and (2) in Scheme 1. The second possible path is through cleavage of an acetylacetonato–metal bond followed by alkene coordination. The third possible path is through an associative mechanism (alkene coordination followed by CO dissociation). (ii) During the process of oxidative addition of H₂, identification of the CO bonding to the metal or dissociating from the metal as H₂ attacks the metal center is crucial in determining the reaction rate. Why should the reaction occur under high pressure of hydrogen? (iii) The regioselectivity for insertion of alkene into Rh–H due to the existence of two hydrides, one *trans* to CO and the other *cis* to CO. (iv) Is the CO occupying the apical position as shown by step 5 in Scheme 1 or instead the hydride occupying the apical position for reductive elimination of the product?

We set out to investigate the detailed reaction mechanisms and probe the catalytic activity of the catalyst with the aid of density functional theory (DFT) calculations. We hope this study could provide valuable information on the reaction and play a guiding role for further designing such kind of new reactions.

2. Computational details

Molecular geometries of all the complexes studied were optimized at the Becke3LYP level of density functional theory [38–41]. Frequency calculations at the same level of theory were also performed to identify all the stationary points as minima (zero imaginary frequencies) or transition states (one imaginary frequency) and to provide free energies at 298.15 K which include entropic contributions by taking into account the vibrational, rotational, and translational motions of the species under

* Corresponding author. Fax: +86 537 4456305.
E-mail address: siweibi@126.com (S. Bi).



Scheme 1.

consideration. The intrinsic reaction coordinate (IRC) [42,43] analysis was carried out to confirm that all stationary points are smoothly connected to each other (see Appendix A, Supplementary data for more details). The lanl2dz basis set [44] was used for Rh atoms and the 6-31G [45] basis set was used for other atoms. Polarization functions were selectively added for C, O and H atoms [$C(\zeta_d = 0.8)$, $O(\zeta_d = 0.8)$ and $H(\zeta_p = 0.11)$], except for those C and H atoms in the acetylacetonato ligands. The effect of solvent was examined by performing single-point self-consistent reaction field (SCRF) calculations based on the polarizable continuum model (PCM) [46–49] for several selected gas-phase-optimized species. Cyclohexane was used as the solvent, corresponding to the experimental conditions, and the atomic radii were used for the PCM calculations. The results show that the solvent effect is small. For example, without the solvation energies, the relative electronic energies of **Cat**, **TS1**, **Int1**, **TS2**, **TS3**, **Int3**, **TS4**, **Int4**, **TS5**, **TS6** and **TS7** are 0.0, 11.9, 9.3, 11.0, 46.6, 39.5, 44.2, 32.7, 34.9, 9.4, and 11.6 kcal/mol, respectively. With the solvation energies included, the relative solvation-corrected electronic energies are 0.0, 12.0, 9.7, 11.5, 46.9, 39.7, 44.3, 32.5, 34.6, 9.5, and 11.9 kcal/mol, respectively. All the DFT calculations were performed with GAUSSIAN 03 packages [50].

3. Results and discussion

All the optimized structures with selected structural parameters for the species involved in this catalytic cycle were presented in Fig. 1 of Appendix A, Supplementary data. The catalyst $\text{Rh}(\text{acac})(\text{CO})_2$ (**Cat**) molecule adopts a square-planar geometry, as expected for rhodium(I) complexes. The calculated structure of the catalyst shown in Fig. 1 of Appendix A, Supplementary data is compared here with its corresponding experimental one. Calculated geometric parameters, $O1-C3 = 1.29 \text{ \AA}$, $O2-C4 = 1.29 \text{ \AA}$, $C1-O3 = 1.15 \text{ \AA}$, $C2-O4 = 1.15 \text{ \AA}$, agree well with the experimentally determined values for the catalyst, $O1-C3 = 1.28 \text{ \AA}$, $O2-C4 = 1.28 \text{ \AA}$, $C1-O3 = 1.14 \text{ \AA}$, $C2-O4 = 1.16 \text{ \AA}$. The rhodium–oxygen and rhodium–carbonyl bonds are very close to the corresponding X-ray crystal structure of $\text{Rh}(\text{acac})(\text{CO})_2$ [51] (bond,

calculated, X-ray crystal): ($\text{Rh}-\text{O}_{\text{acac}}$, $2.06/2.06 \text{ \AA}$, $2.04/2.04 \text{ \AA}$) and ($\text{Rh}-\text{C}$, $1.88/1.88 \text{ \AA}$, $1.82/1.83 \text{ \AA}$). These small deviations in the metal–ligand bond lengths are not considered critical here [52]. Thus it can be confirmed that the basis sets are adequate for present study.

In view of the fact that the relative free energies and relative electronic energies differ significantly in cases where the number of reactant and product molecules is different because of the entropic contributions, free energies are used in this paper to analyze the reaction mechanism due to one-to-two or two-to-one transformations involved in the proposed catalytic cycle. In this study, the experimental catalyst $\text{Rh}(\text{acac})(\text{CO})_2$ and ethene (one of the experimental alkenes) are employed for the detailed exploration of alkene hydrogenation.

3.1. C_2H_4 coordination by substitution

Substitution reactions of square-planar low-spin d^8 compounds such as group 9 and group 10 complexes have been investigated both experimentally [53–56] and theoretically [57–59]. A few examples of dissociative substitution have been reported for rhodium(I) and platinum(II) complexes [60,61] but most substitution reactions at square-planar low-spin d^8 systems seem to occur through an interchange mechanism [62] (involving formation of a single trigonal-bipyramidal transition state) or an associative mechanism [62] (involving two transition states separated by a trigonal-bipyramidal intermediate) [57–59]. Hopmann studied the substitution reaction of $\text{Rh}(\text{acac})(\text{CO})_2$ with PPh_3 , and found the substitution mechanism was different from the three ones mentioned above [63]. Prior to dissociation of CO, attack of PPh_3 on $\text{Rh}(\text{acac})(\text{CO})_2$ first results in cleavage of an acetylacetonato bond and leads to formation of a square-planar intermediate.

As for the substitution reaction of $\text{Rh}(\text{acac})(\text{CO})_2$ with alkene, Zhang and co-workers proposed a dissociative mechanism as shown in Scheme 1, involving dissociation of a CO ligand to give a three-coordinate T-shape intermediate, followed by coordination of alkene. Considering strong interaction of Rh–CO, the substitution mechanisms need to be further investigated. Three possible pathways are proposed for the substitution process as shown in Fig. 1, together with calculated free energies and electronic energies (in parentheses). The first two pathways are dissociative processes, one (Fig. 1a) corresponding to loss of CO and the other (Fig. 1b) to cleavage of an acetylacetonato bond. The third pathway (Fig. 1c) is an associative process where ethene first binds to the catalyst to afford an intermediate (**Int1**) followed by release of CO. The first path associated with transformation of the four-coordinate $\text{Rh}(\text{acac})(\text{CO})_2$ complex into separated fragments, that is, the three-coordinate $\text{Rh}(\text{acac})(\text{CO})$ complex and free CO (Fig. 1a), is found to be barrierless. The free energy and electronic energy differences are calculated to be very high (ΔG : 34.0 kcal/mol and ΔE : 46.6 kcal/mol). For the second path involving cleavage of a $\text{Rh}-\text{O}_{\text{acac}}$ bond, the free energies and electronic energies of the transition state (**TSb**) and the intermediate (**Intb**) are still very high (see Fig. 1b). Thus, the third pathway becomes necessary for examination.

As shown in Fig. 1c, the last pathway is proposed to be an associative process. The first step is the coordination of ethene to Rh center to afford an intermediate **Int1** via the transition state **TS1** with a free energy barrier of 18.0 kcal/mol. **TS1** is found to have a pseudotrigonal bipyramidal (TBP) structure. The angle for the three axial atoms $C1-\text{Rh}-O2_{\text{acac}}$ is 179.4° . The three angles in the equatorial plane, $C2-\text{Rh}-O1_{\text{acac}}$, $C2-\text{Rh}$ –(centroid of ethene) and $O1_{\text{acac}}-\text{Rh}$ –(centroid of ethene) are 132.8° , 130.2° and 96.5° , respectively. The geometric structure of this transition state is similar to the one with a phosphine ligand PPh_3 attacking the Rh center [63]. However, we found the geometric structure of **Int1**

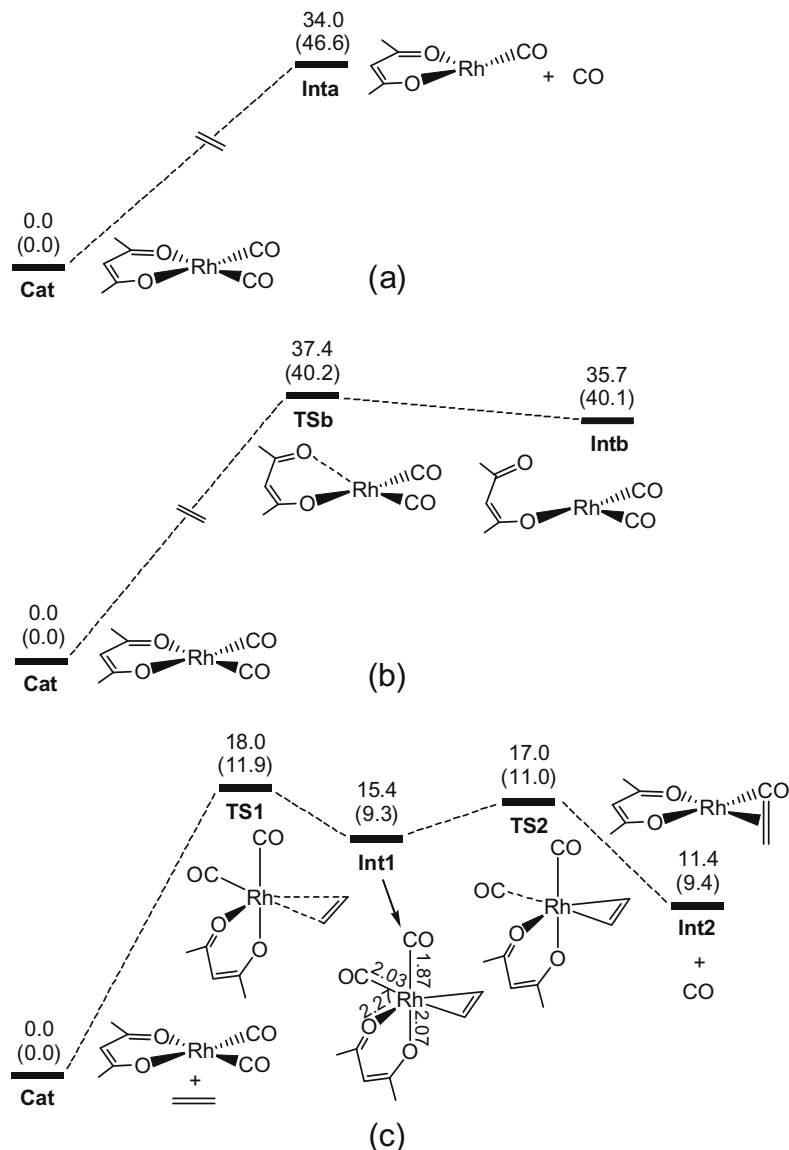


Fig. 1. Free energy profile calculated for the substitution of CO by ethene. The relative free energies and electronic energies (in parentheses) are given in kcal/mol.

obtained from **TS1** is different from the one obtained from the coordination of PPh_3 to the same catalyst ($\text{Rh}(\text{acac})(\text{CO})_2$). **Int1** is pseudotrigonal bipyramidal supported by the data shown in Fig. 1 of Appendix A, Supplementary data, while the intermediate with a PPh_3 was found to be square-planar with the O_{acac} corresponding to O1_{acac} in **Int1** completely away from the Rh center [63]. That implies ethene has less ability than PPh_3 for pushing the equatorial oxygen away from Rh center. The following step is release of a CO ligand. There are two possible modes for release of a CO. One is the release of the equatorial CO and the other is the release of the axial CO. The former mode is predicted to be preferred over the latter one [58,64]. For such a d^8 TBP complex, the highest two HOMOs lie in the equatorial plane and have antibonding character, thus leading to a weaker equatorial than an axial M–L linkage [65]. As the calculated results show, the equatorial Rh–C (2.03 Å) is longer than the axial Rh–C (1.87 Å). Also, the equatorial Rh– O_{acac} (2.27 Å) is longer than the axial Rh– O_{acac} (2.07 Å). The free energy barrier for release of the equatorial CO from **Int1** is calculated to be only 1.6 kcal/mol, and the free energy difference from **Int1** to **Int2** is –4.0 kcal/mol. For the substitution process from **Cat** to **Int2**, the free energy difference is 11.4 kcal/mol, indicate this

process is thermodynamically unfavorable. Therefore, the substitution can be completed only under the presence of a considerable quantity of alkene and the absence of carbon monoxide, which is consistent with the experimental facts [37]. Experiments also found that introducing CO into the $\text{Rh}(\text{acac})(\text{CO})(\text{alkene})$ results in a rapid disappearance of **Int2** and the regeneration of **Cat** [37]. This phenomenon can be well explained by using the reverse process from **Int2** to **Cat** as shown in Fig. 1c. The exothermicity (–11.4 kcal/mol) and the low free energy barrier where the highest barrier is only 6.6 kcal/mol relevant to **Int2** for the reverse process indicate this process is much favorable both thermodynamically and kinetically. In summary, an associative mechanism is found to be preferred over the dissociative mechanism for the substitution of CO by ethene.

3.2. Oxidative addition of H_2

The free energy profile calculated for oxidative addition of H_2 is shown in Fig. 2a. The first step is the coordination of H_2 to afford a non-classical σ -complex (**Int3**) through **TS3**. The long Rh–CO bond distance (3.25 Å) in **Int3** indicates that the CO ligand is almost

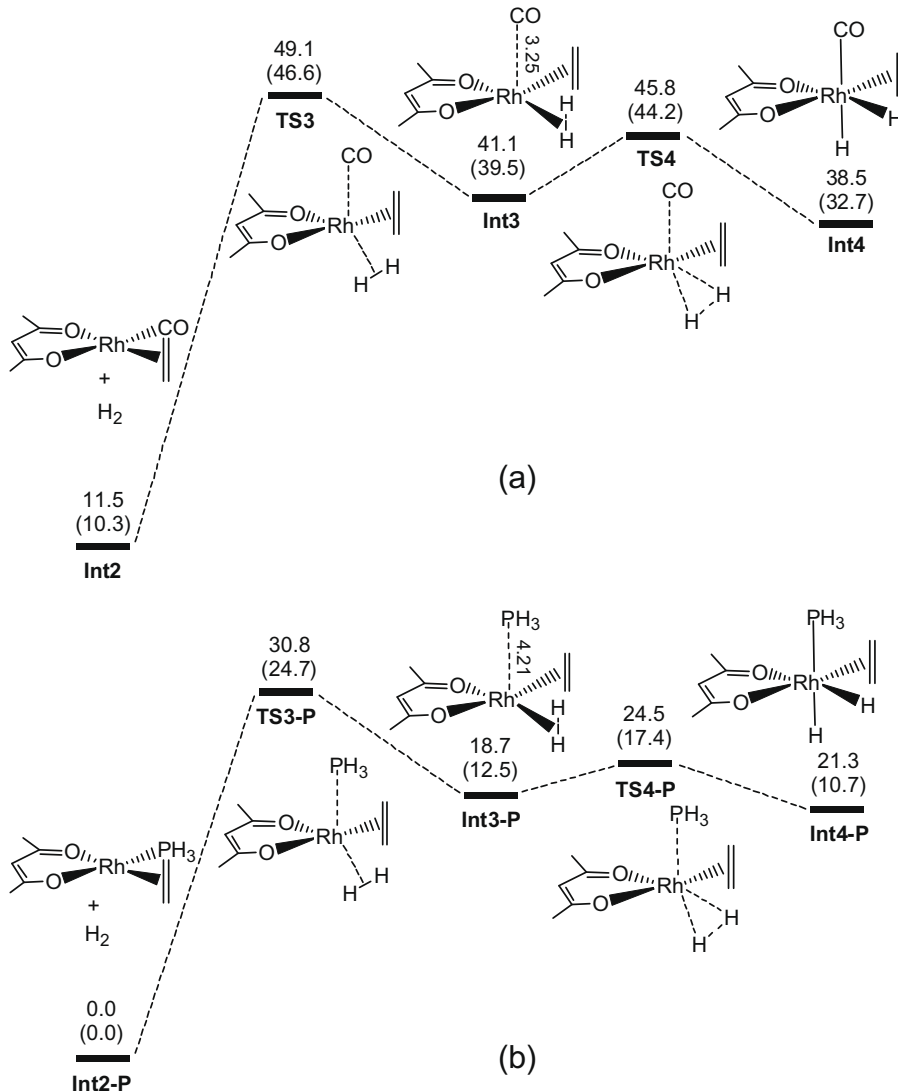


Fig. 2. Free energy profile calculated for oxidative addition of H₂. The relative free energies and electronic energies (in parentheses) are given in kcal/mol.

dissociated from the metal center, and thus the fragment Rh-(acac)(C₂H₄)(H₂) adopts a square planar structure. Instead, a five-coordinate trigonal bipyramidal structure cannot be located. This step can be regarded as a substitution of a CO ligand by H₂. The following step is the oxidative addition of H₂ to give a bishydrido complex (Int4). Small activation barrier (4.7 kcal/mol) indicates this step is facile and the exothermicity confirms this step is thermodynamically favorable. It is to note that Int3 and Int4 are much higher than Int2, correspondingly making the TS3 and TS4 to be also very high in energy. Therefore, the oxidative addition of H₂ is clearly very unfavorable both thermodynamically and kinetically. The results of calculations are in accordance with the experimental facts that the reactions for hydrogenation of alkene catalyzed by the catalyst Rh(acac)(CO)₂ proceed under high pressure of H₂ [37]. The reason for the difficulty of oxidative addition of H₂ is originated from the substitution step (Int2 to Int3), since in this step the strong Rh-CO bond is broken while only a weak Rh-(η^2 -H₂) bond is formed. In other words, the bonding strength of the coligand such as CO determines the degree of difficulty for oxidative addition of H₂. The weaker the M-L (L: acting as coligand, such as CO as mentioned above), the easier for oxidative addition of H₂. For example, we replaced the CO by a PH₃ ligand to estimate the kinetics and thermodynamics for oxidative addition of H₂ as

shown in Fig. 2b. The path is similar to the one shown in Fig. 2a. In Int3-P, PH₃ nearly dissociates from the metal center, thus resulting in substitution of PH₃ by H₂. We respectively, calculated the binding energies of PH₃ and CO with the fragment Rh(acac)(C₂H₄), and found the former (29.4 kcal/mol) is smaller than the latter (44.1 kcal/mol). As a result, the substitution of PH₃ is easier than that of CO. The free energies of TS3, Int3, TS4 and Int4 relative to Int2 are 37.6, 29.6, 34.3 and 27.0 kcal/mol, while those of TS3-P, Int3-P, TS4-P and Int4-P relative to Int2-P are 30.8, 18.7, 24.5 and 21.3 kcal/mol. In summary, in the process of oxidative addition of H₂ the substitution step of H₂ by CO first takes place, which makes the Rh-CO broken and leads to the process being difficult.

3.3. Insertion ethene into Rh-H

There are two modes for the insertion of ethene into the Rh-H bond, one into the Rh-H trans to the CO ligand, and the other into the Rh-H cis to the CO ligand. The free energy profiles are shown in Fig. 3. If ethene inserts into the Rh-H trans to the CO ligand, the located transition state TS5 connects Int4 and Int5. If the ethene inserts into the Rh-H cis to the CO ligand, the located transition state TS5' connects Int4' and Int5'. Ethene is found to be parallel to Rh-CO in TS5, and perpendicular to Rh-CO in TS5'. Clearly, if the

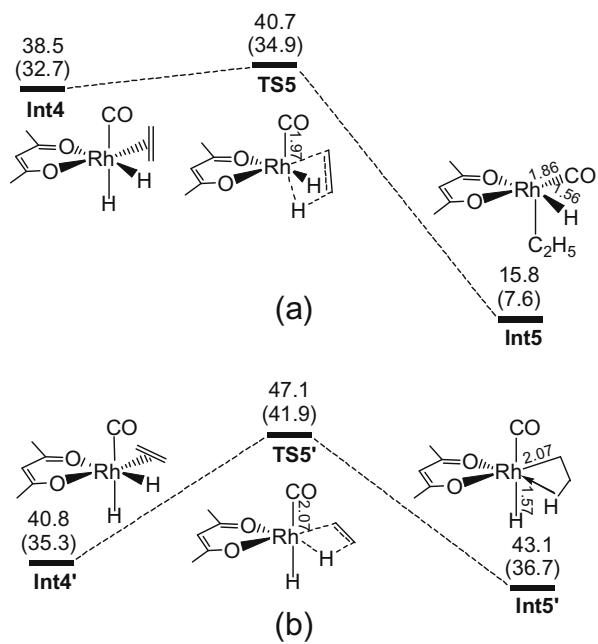


Fig. 3. Free energy profile calculated for ethene insertion into M–H bond. The relative free energies and electronic energies (in parentheses) are given in kcal/mol.

reaction goes through the path including **Int4'** and **Int5'**, a prior isomerization from **Int4** and **Int4'** is needed. **TS5** becomes more stable than **TS5'** as a result of decreased CO–Rh–H trans influence. As calculated results show, the Rh–CO in **TS5** (1.97 Å) is noticeably shorter than that in **TS5'** (2.07 Å). **Int5** is much more stable than **Int5'**, which is clearly due to the disappearance of the strong CO–Rh–H trans influence in **Int5**. In **Int5** and **Int5'**, the calculated Rh–CO bond distances are 1.86 Å and 2.07 Å, and those of Rh–H are 1.56 Å and 1.57 Å, respectively. In view of the fact that **TS5** is more stable than **TS5'**, the path from **Int4** to **Int5** is preferred over the one from **Int4'** to **Int5'**.

3.4. Reductive elimination of ethane

Two possible paths were proposed for reductive elimination of ethane from **Int5**. As shown in Fig. 4, the first path (a) is related to the direct reductive elimination of ethane from **Int5**. The second path (b) tells that **Int5** first binds with a CO ligand to give more stable 18e intermediate (**Int6'**), and then reductive elimination of ethane is followed.

For reductive elimination of ethane from **Int5** in Fig. 4a, we cannot locate a transition state directly connecting **Int5** and **Int7**. Instead, a transition state (**TS7**) is always located connecting **Int6** and **Int7**, which is similar to the cases reported by literatures [66,67]. In **Int6**, the hydride occupies the pyramidal position. Thus, before the reductive elimination takes place, **Int5** should first

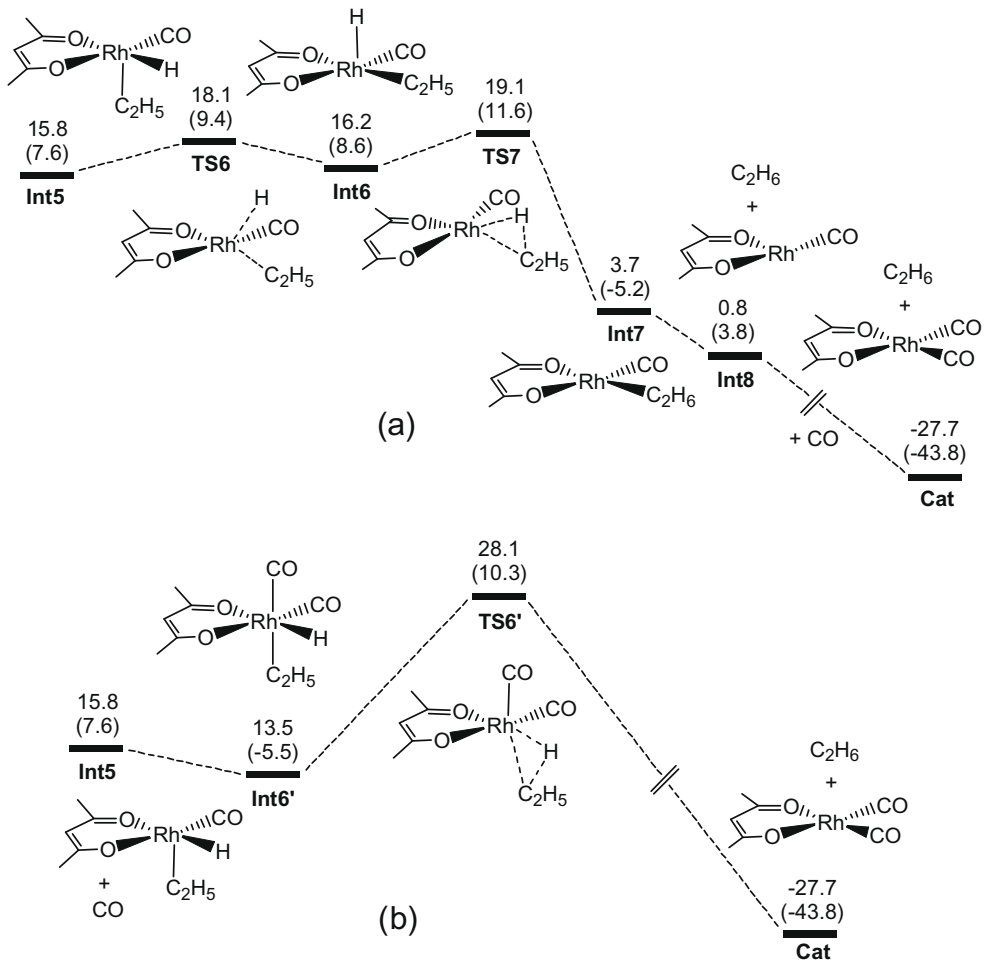
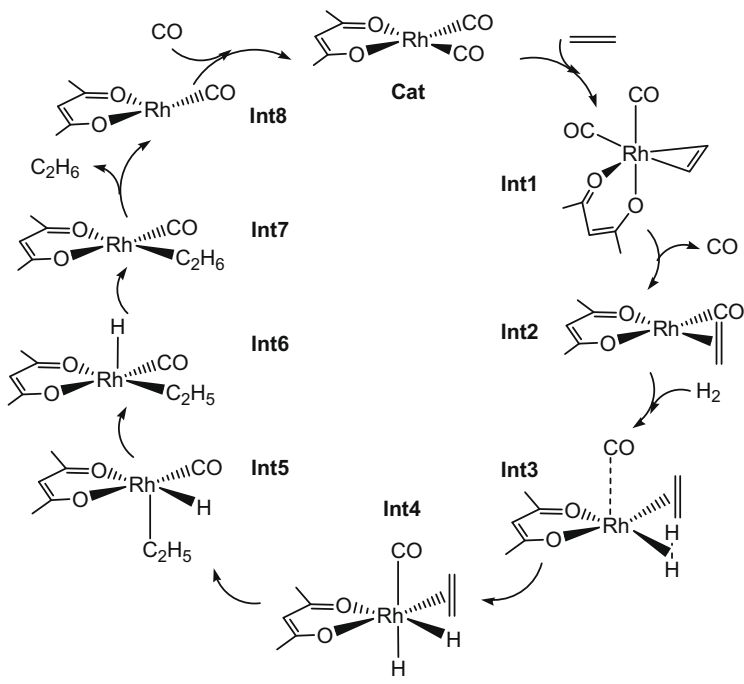


Fig. 4. Free energy profile calculated for reductive elimination of ethane. The relative free energies and electronic energies (in parentheses) are given in kcal/mol.



Scheme 2.

isomerize to **Int6**. It is found the free activation energy for reductive elimination of ethane (**Int6** to **Int7**) is only 2.9 kcal/mol and the free energy difference for the step is 12.5 kcal/mol, indicating much favorable kinetically and thermodynamically. The step from **Int7** to **Int8** is the release of ethane from the metal center. The driving force for the step is mainly the contribution of entropy increase. Experiments confirmed the existence of $\text{Rh}(\text{acac})(\text{CO})$ [37], agreeing with our theoretical predication. The last step is the coordination of CO to $\text{Rh}(\text{acac})(\text{CO})$ to regenerate the catalyst.

In the second path (Fig. 4b), the coordination of CO to **Int5** gives a more stable six-coordinate 18e intermediate (**Int6'**). However, the reductive elimination of ethane from **Int6'** is found to be less favorable kinetically with a free activation barrier of 14.6 kcal/mol, even though this step can directly produce the product ethane and regenerate the catalyst. This in turn indicates that the octahedral d^6 complex (**Int6'**) prefers to undergo reductive elimination with initial loss of CO to generate the more reactive intermediate **Int5** [66,67]. On the basis of our calculations and analyses, the catalytic cycle for hydrogenation of ethene catalyzed by $\text{Rh}(\text{acac})(\text{CO})_2$ can be drawn in Scheme 2.

4. Conclusions

The reaction mechanisms on hydrogenation of ethene catalyzed by $\text{Rh}(\text{acac})(\text{CO})_2$ has been investigated with the aid of density functional calculations. It can be drawn from this work as follows:

- (1) For the substitution of a CO of the catalyst by ethene, the associative mechanism (**Cat** to **Int2**) is found to be preferred over the dissociative one. That is, the catalyst rather undergoes coordination of ethene to the catalyst to give a five-coordinate 18e intermediate than undergoes breaking of the bond Rh–CO or Rh–O_{acac} to give a three-coordinate 14e intermediate, since the Rh–CO and Rh–O_{acac} are very strong.
- (2) For the process of the oxidative addition of H₂ (**Int2** to **Int4**), a substitution step (**Int2** to **Int3**) is found to occur firstly, resulting in the breaking of the Rh–CO bond and making the step very unfavorable both in kinetics and

thermodynamics. The high pressure of H₂ used in experiments is in accordance with our prediction. This step is predicted to be the key step in determining the reaction rate. If the coordinated CO is replaced by a relatively weak ligand, the substitution process would become more favorable.

- (3) For insertion of ethene into the Rh–H, the path for insertion into the Rh–H trans to Rh–CO is preferred over the one into the Rh–H cis to Rh–CO since the trans influence of CO–Rh–H decreases significantly in **TS5** and **Int5** of the former path.
- (4) Reductive elimination of ethane directly from the square-pyramidal 16e $\text{RhH}(\text{acac})(\text{CO})(\text{C}_2\text{H}_5)$ (**Int5**) is found to be more favorable than the one from the octahedral 18e $\text{RhH}(\text{acac})(\text{CO})_2(\text{C}_2\text{H}_5)$ (**Int6'**).

Acknowledgments

This work was supported by the Natural Science Foundation of Shandong Province (No. Y2007B23), the State Key Laboratory of Physical Chemistry of Solid Surfaces, Xiamen University, China (No. 200702), and the Key Laboratory of Colloid Interface Chemistry, Ministry of Education, Shandong University (No. 200706).

Appendix A. Supplementary material

Supplementary data associated with this article can be found, in the online version, at [doi:10.1016/j.jorgchem.2010.03.015](https://doi.org/10.1016/j.jorgchem.2010.03.015).

References

- [1] J.A. Belmont, J. Soto, R.E. King, A.J. Donaldson, J.D. Hewes, M.F. Hawthorne, *J. Am. Chem. Soc.* 111 (1989) 7475–7486.
- [2] P.E. Behnken, J.A. Belmont, D.C. Busby, M.S. Delaney, R.E. King, C.W. Kreinendahl, T.B. Marder, J.J. Wilczynski, M.F. Hawthorne, *J. Am. Chem. Soc.* 106 (1984) 3011–3025.
- [3] R.L. Hoenigman, S. Kato, V.M. Bierbaum, W.T. Borden, *J. Am. Chem. Soc.* 127 (2005) 17772–17777.
- [4] A. Alvarez, R. Macias, J. Bould, M.J. Fabra, F.J. Lahoz, L.A. Oro, *J. Am. Chem. Soc.* 130 (2008) 11455–11466.

[5] F. Teixidor, M.A. Flores, C. Vinas, R. Sillanpaa, R. Kivekas, *J. Am. Chem. Soc.* 122 (2000) 1963–1973.

[6] M.J. Clarke, A.I. Cooper, S.M. Howdle, M. Poliakoff, *J. Am. Chem. Soc.* 122 (2000) 2523–2531.

[7] B.E. Maryanoff, H.R. Almond Jr., *J. Org. Chem.* 51 (1986) 3295–3302.

[8] O.S. Alexeev, F. Li, M.D. Amiridis, B.C. Gates, *J. Phys. Chem. B* 109 (2005) 2338–2349.

[9] M.S. Kwon, N. Kim, C.M. Park, J.S. Lee, K.Y. Kang, J. Park, *Org. Lett.* 7 (2005) 1077–1079.

[10] H.M. Lee, T. Jiang, E.D. Stevens, S.P. Nolan, *Organometallics* 20 (2001) 1255–1258.

[11] A. Rifat, N.J. Patmore, M.F. Mahon, A.S. Weller, *Organometallics* 21 (2002) 2856–2865.

[12] J. Cipot, R. McDonald, M. Stradiotto, *Organometallics* 25 (2006) 29–31.

[13] R.J. Trovitch, E. Lobkovsky, E. Bill, P.J. Chirik, *Organometallics* 27 (2008) 1470–1478.

[14] C. Vinas, M.A. Flores, R. Nunez, F. Teixidor, R. Kivekas, R. Sillanpaa, *Organometallics* 17 (1998) 2278–2289.

[15] K.D. Hesp, D. Wechsler, J. Cipot, A. Myers, R. McDonald, M.J. Ferguson, G. Schatte, M. Stradiotto, *Organometallics* 26 (2007) 5430–5437.

[16] F.H. Antwi-Nsiah, J.R. Torkelson, M. Cowie, *Inorg. Chim. Acta* 259 (1997) 213–226.

[17] C. Pettinari, F. Marchetti, D. Martini, In: J.A. McCleverty, T.J. Meyer (Eds.), *Comprehensive Coordination Chemistry II*, Elsevier, Oxford, UK, 2004 (Chapter 9).

[18] F.W. Grevels, J. Jacke, S. Ozkar, *J. Am. Chem. Soc.* 109 (1987) 7536–7537.

[19] J.M. Zhuang, D. Sutton, *Organometallics* 10 (1991) 1516–1527.

[20] Y.-X. He, R.J. Batchelor, F.W.B. Einstein, D. Sutton, *J. Organomet. Chem.* 509 (1996) 37–48.

[21] P.W. Dyer, V.C. Gibson, W. Clegg, *J. Chem. Soc. Dalton Trans.* (1995) 3313–3316.

[22] J.A. Banister, P.D. Lee, M. Poliakoff, *Organometallics* 14 (1995) 3876–3885.

[23] J.A. Banister, S.M. Howdle, M. Poliakoff, *J. Chem. Soc. Chem. Commun.* (1993) 1814–1815.

[24] J.L. King, K. Molvinger, M. Poliakoff, *Organometallics* 19 (2000) 5077–5082.

[25] M.J. Hostetler, M.D. Butts, R.G. Bergman, *J. Am. Chem. Soc.* 115 (1993) 2743–2752.

[26] P.A. Chaloner, M.A. Esteruelas, F. Joo, L.A. Oro, *Homogeneous Hydrogenation*, Kluwer Academic Publishers, Dordrecht, The Netherlands, 1994.

[27] J. Yu, J.B. Spencer, *J. Am. Chem. Soc.* 119 (1997) 5257–5258.

[28] C. Deibebe, A.B. Permin, V.S. Petrosyan, J. Bargon, *Eur. J. Inorg. Chem.* 12 (1998) 1915–1923.

[29] R.A. Sanchez-Delgado, M. Rosales, *Coord. Chem. Rev.* 196 (2000) 249–280.

[30] S. Lange, W. Leitner, *J. Chem. Soc. Dalton Trans.* (2002) 752–758.

[31] E. Mieczynska, A.M. Trzeciak, J.J. Ziolkowski, *J. Mol. Catal.* 80 (1993) 189–200.

[32] A.M. Trzeciak, M. Mieczynska, J.J. Ziolkowski, *Top. Catal.* 11/12 (2000) 461–468.

[33] H. Jin, B. Subramaniam, A. Ghosh, J. Tunge, *AIChE J.* 52 (2006) 2575–2581.

[34] J. Zhang, M. Poliakoff, M.W. George, *Organometallics* 22 (2003) 1612–1618.

[35] F. Bonati, G. Wilkinson, *J. Chem. Soc.* (1964) 3156–3160.

[36] A.S. Berenblyum, M.V. Ermolaev, I.V. Kalechits, L.I. Lakhman, M.L. Khidekel, All-Union Scientific-Research Institute of Petroleum Refining, Su, USSR, 1974.

[37] J. Zhang, X.-Z. Sun, M. Poliakoff, M.W. George, *J. Organomet. Chem.* 678 (2003) 128–133.

[38] A.D. Becke, *J. Chem. Phys.* 98 (1993) 5648–5652.

[39] P.J. Stephens, F.J. Devlin, C.F. Chabalowski, M.J. Frisch, *J. Phys. Chem.* 98 (1994) 11623–11627.

[40] B. Miehlich, A. Savin, H. Stoll, H. Preuss, *Chem. Phys. Lett.* 157 (1989) 200–206.

[41] C. Lee, W. Yang, R.G. Parr, *Phys. Rev. B* 37 (1988) 785–789.

[42] K. Fukui, *J. Phys. Chem.* 74 (1970) 4161–4163.

[43] K. Fukui, *Acc. Chem. Res.* 14 (1981) 363–368.

[44] R. Krishnan, J.S. Binkley, R. Seeger, J.A. Pople, *J. Chem. Phys.* 72 (1980) 650–654.

[45] P.C. Hariharan, J.A. Pople, *Theor. Chim. Acta* 28 (1973) 213–221.

[46] V. Barone, M. Cossi, *Phys. Chem. A* 102 (1998) 1995–2001.

[47] M. Cossi, N. Rega, G. Scalmani, V. Barone, *J. Comput. Chem.* 24 (2003) 669–681.

[48] J. Tomasi, B. Mennucci, R. Cammi, *Chem. Rev.* 105 (2005) 2999–3094.

[49] S. Miertus, E. Scrocco, J. Tomasi, *Chem. Phys.* 55 (1981) 117–129.

[50] M.J. Frisch, et al., *GAUSSIAN 03*, revision B05, *GAUSSIAN, inc.*, Pittsburgh, PA, 2003.

[51] F. Huq, A.C. Skapski, *J. Cryst. Mol. Struct.* 4 (1974) 411–413.

[52] W.J. Hehre, *A Guide to Molecular Mechanisms and Quantum: Chemical Calculations*, Wavefunction Inc., Irvine, CA, 2003, pp. 153–181.

[53] S. Serron, J. Huang, S.P. Nolan, *Organometallics* 17 (1998) 534–539.

[54] R. van Eldik, S. Aygen, H. Kelm, A.M. Trzeciak, J.J. Ziolkowski, *Transition Met. Chem.* 10 (1985) 167–171.

[55] W. Simanko, K. Mereiter, R. Schmid, K. Kirchner, A.M. Trzeciak, J. Ziolkowski, *J. Organomet. Chem.* 602 (2000) 59–64.

[56] R.J. Mureinik, *Coord. Chem. Rev.* 25 (1978) 1–30.

[57] J. Cooper, T. Ziegler, *Inorg. Chem.* 41 (2002) 6614–6622.

[58] Z. Lin, M.B. Hall, *Inorg. Chem.* 30 (1991) 646–651.

[59] J.K. Burdett, *Inorg. Chem.* 16 (1977) 3013–3025.

[60] R.E. Bossio, T.N.W. Hoffman, T.R. Cundari, A.G. Marshall, *Organometallics* 23 (2004) 144–148.

[61] R. Romeo, S.L. Monsu, M.R. Plutino, D.B.F. Fabrizi, G. Bottari, A. Romeo, *Inorg. Chim. Acta* 350 (2003) 143–151.

[62] C.E. Housecroft, A.G. Sharpe, *Inorganic Chemistry*, second ed., Pearson Education Limited, 2005.

[63] K.H. Hopmann, J. Conradie, *Organometallics* 28 (2009) 3710–3715.

[64] R.H. Crabtree, *The organometallic chemistry of the transition metals. A Comprehensive Introduction to Principles and Practices*, 3rd ed., John Wiley and Sons, Inc., New York, 2001, pp. 100–101.

[65] T.A. Albright, J.K. Burdett, M.-H. Whangbo, *Orbital Interactions in Chemistry, A Guide to Understanding the Molecular Orbital Calculations*, John Wiley and Sons, Inc., 1985, pp. 317–320.

[66] D. Milstein, *Acc. Chem. Res.* 17 (1984) 221–224.

[67] R.H. Crabtree, *The organometallic chemistry of the transition metals. A Comprehensive Introduction to Principles and Practices*, third ed., John Wiley and Sons, Inc., New York, 2001, pp. 162–163.